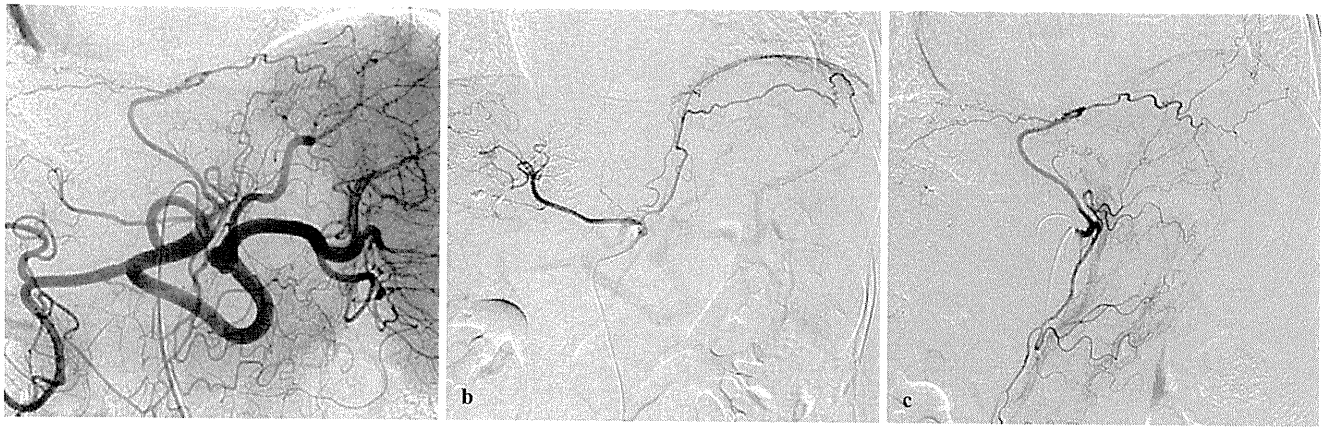


**Fig. 12.** **a** Celiac arteriogram. **b** Anterior branch of the left IPA arises with the right IPA as a common trunk from the celiac artery. **c** Posterior branch of the left IPA arises from the left gastric artery

**Fig. 13.** Right IPA communicates with the pericardiacophrenic artery arising from the right internal mammary artery (*arrow*). Vascular blush caused by a transpleural systemic–pulmonary arterial anastomosis from the left IPA is also seen (*arrowhead*)

eterization into several types of IPA remains impossible even using a conventional coaxial technique. An IPA that arises from the proximal portion of the celiac trunk or from the aorta with an acute angle at the orifice is difficult to catheterize. Using a catheter with a large side hole or turn-back technique is useful when selecting IPAs arising from the proximal portion of the celiac trunk.[8,9] For IPAs arising from the aorta with an acute angle, a catheter with a cleft facilitates catheterization (Fig. 19).[10] Both the large side hole and the cleft can easily be created on a conventional angiographic catheter during the procedure according to the individual circumstances.[8,10] In addition, selective catheterization into the IPA arising from the distal portion of the celiac trunk is frequently difficult because the tip of the angiographic catheter does not closely face the IPA orifice. For selective catheterization into such IPAs, a catheter with a large side hole is useful (Fig. 20). Shaping a non-braided microcatheter by steam-heating is also useful for selective catheterization.

For TACE through a reconstructed IPA supplying an HCC, selection of a less tortuous root is key to successful catheterization and TACE when the IPA is demonstrated through more than two separate arteries. The anastomotic branch should be selected using a microcatheter with a tip of less than 2F because the anastomotic branch is usually small and tortuous. When the anastomotic branch cannot be directly selected, embolization of the parent artery using metallic coils at a level distal to the anastomotic branch is also useful for avoiding nontarget embolization (Fig. 14).[6]

Direct catheterization into the stenotic vessel is possible in some cases when the IPA orifice can be demonstrated during the TACE procedure (Fig. 15).[14]

## TACE techniques to avoid complications

The gastric and esophageal branches of the IPA should not be embolized. Inflow of embolic material into the pulmonary vessels through the shunt may cause pleural effusion, basal atelectasis, and infrequently systemic embolization. Patients with advanced liver disease are likely to have a pulmonary arteriovenous shunt; and a right-to-left shunt from the IPA to the pulmonary vasculature is a possible route causing cerebral embolism of iodized oil,[15] a rare but severe complication of TACE. Therefore, the tumor-feeding branch should be selectively embolized when obvious pleural and pulmonary staining is demonstrated (Fig. 21). Embolization of the branch toward the pleural and pulmonary staining using metallic coils before TACE is useful if the tumor-feeding

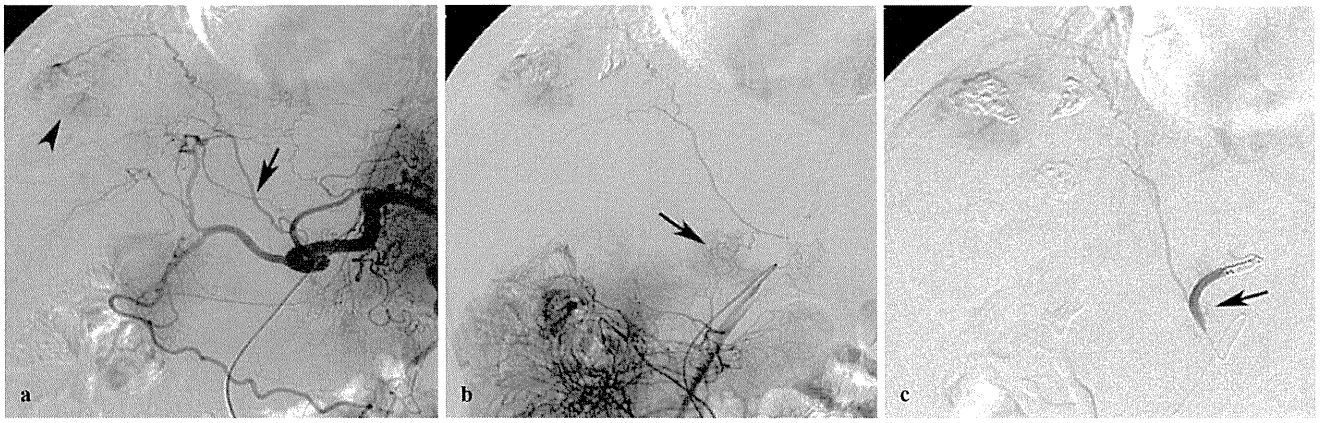


**Fig. 14.** **a** Celiac arteriography shows a tumor stain (*arrowhead*) supplied by the reconstructed right IPA through the left gastric artery (*arrow*). **b** Superior mesenteric arteriography also shows the reconstructed right IPA through the dorsal pancreatic artery (*arrow*). Because the anastomotic branch derived from the dorsal pancreatic artery was tortuous, catheterization through the left gastric artery was attempted. However, catheterization into the anastomotic branch was impossible because of acute angle branching. **c** TACE was performed after coil embolization of the left gastric artery distal to the anastomotic branch. *Arrow* indicates the anastomotic branch

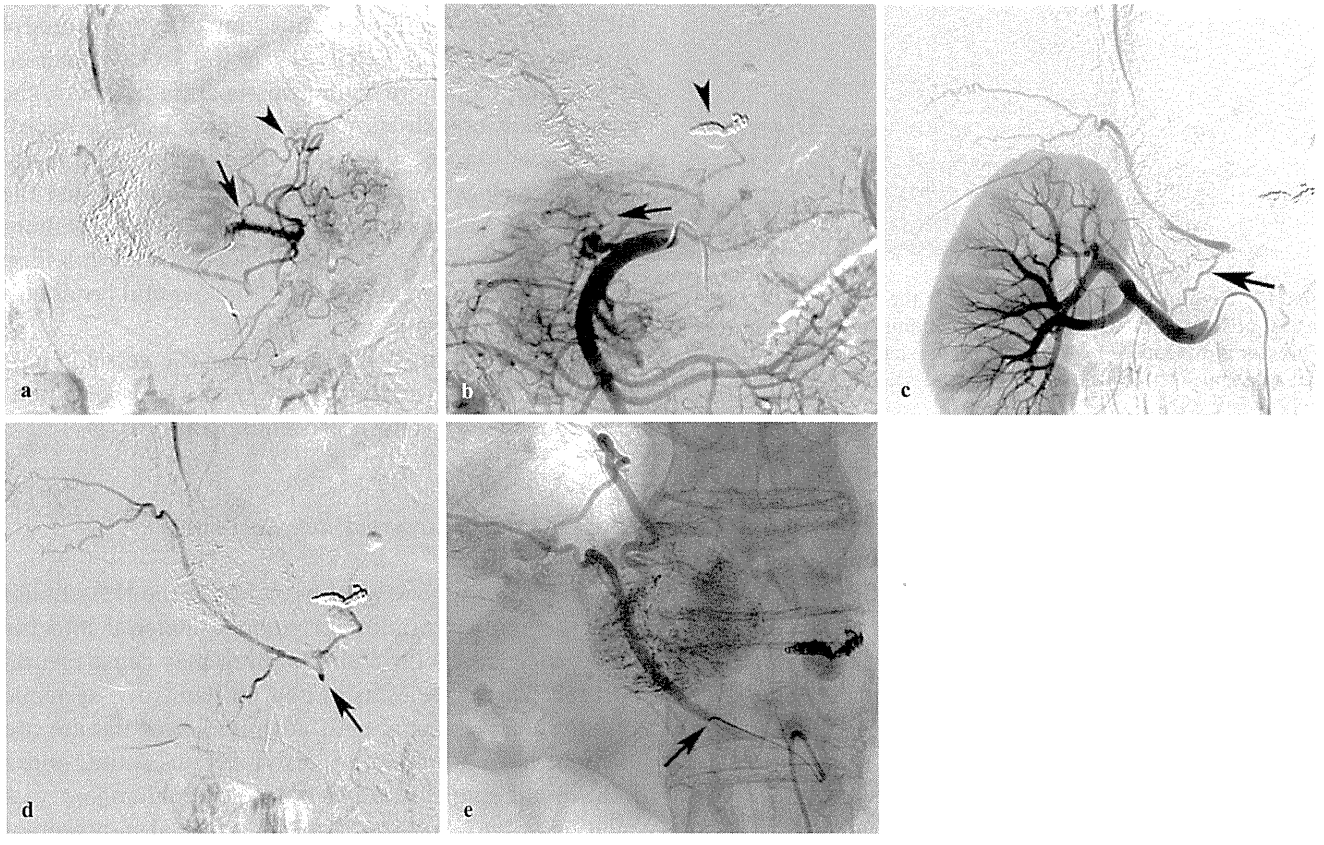


**Fig. 15.** **a** Arteriography of the left gastric artery shows a tumor-feeding branch (*arrow*) and an anastomotic branch between the left gastric artery and the left IPA (*arrowhead*). TACE was performed after coil embolization of the left gastric artery distal to the tumor-feeding branch (not shown). **b** Bilateral IPAs are opacified through the dorsal pancreatic artery (*arrow*) derived from the superior mesenteric artery obtained after TACE of the left gastric artery. *Arrowhead* indicates the metallic coils in the left gastric artery. **c** Right IPA is also opacified through the right inferior adrenal artery (*arrow*). **d** This anastomotic branch was selected, and TACE was performed. During TACE, the stenosed orifice of the common trunk of the bilateral IPAs was demonstrated (*arrow*). **e** Selective catheterization into the stenosed orifice of the common trunk was possible. *Arrow* indicates the catheter tip

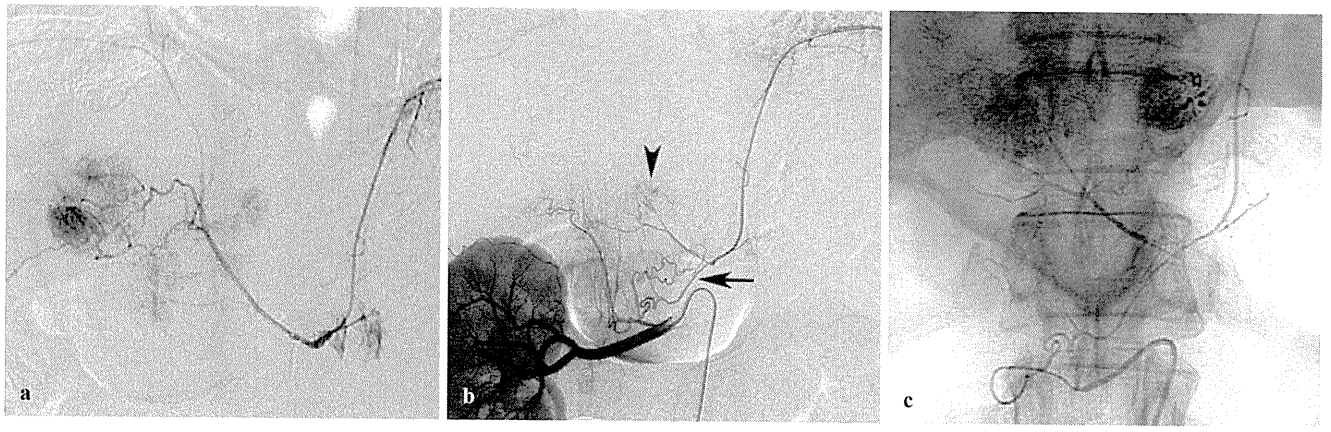


**Fig. 16.** **a** Tumor in the caudate lobe of the liver is supplied by the right IPA arising from the aorta. TACE was performed through the right IPA. **b** At 2 years 1 month later, the tumor has recurred (*arrowhead*), supplied by the reconstructed right IPA through the right inferior adrenal artery (*arrow*). **c** Spot radiograph obtained during the procedure. The anastomotic branch was selected, and TACE was performed

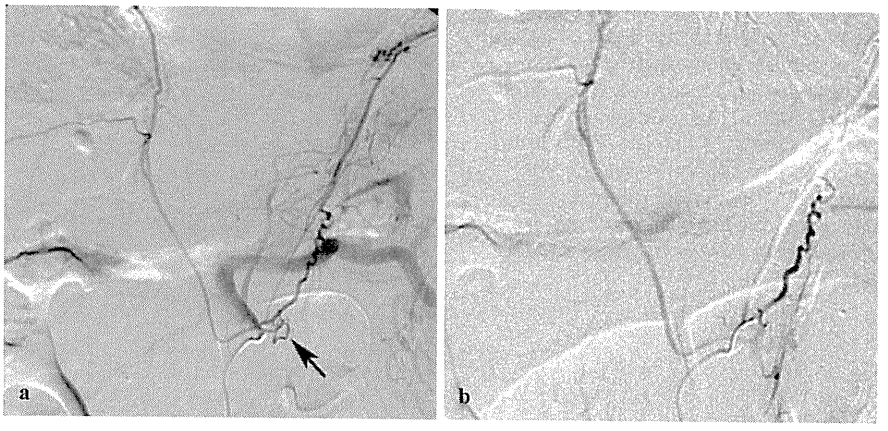


**Fig. 17.** **a** Bilateral IPAs are reconstructed through a small branch arising from the celiac trunk (*arrow*). **b** The branch is successfully selected

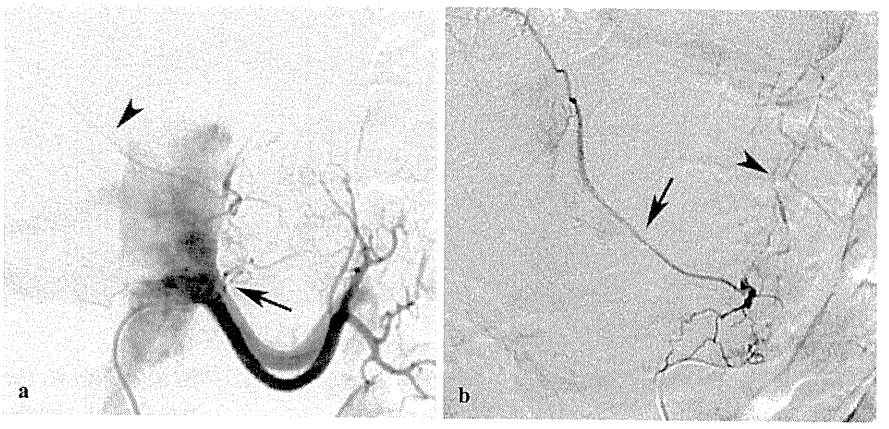


**Fig. 18.** **a** Arteriography of the left renal artery shows that the right IPA (*arrowhead*) is opacified through a small branch arising at the proximal portion (*arrow*). **b** Selective arteriography of the branch shows the right IPA (*arrow*) and gastric branch (*arrowhead*) through a retroperitoneal fine network

branch cannot be selected (Fig. 22). Bland embolization without iodized oil and anticancer drugs is a less risky alternative.

Embolic materials injected with slight force at the distal level may flow into the other extrahepatic collateral vessels through the anastomosis and may cause unexpected nontarget embolization.[16] Careful observation is needed during injection of embolic materials. In addition, the dosage of infused iodized oil and anticancer drugs should be properly reduced compared with

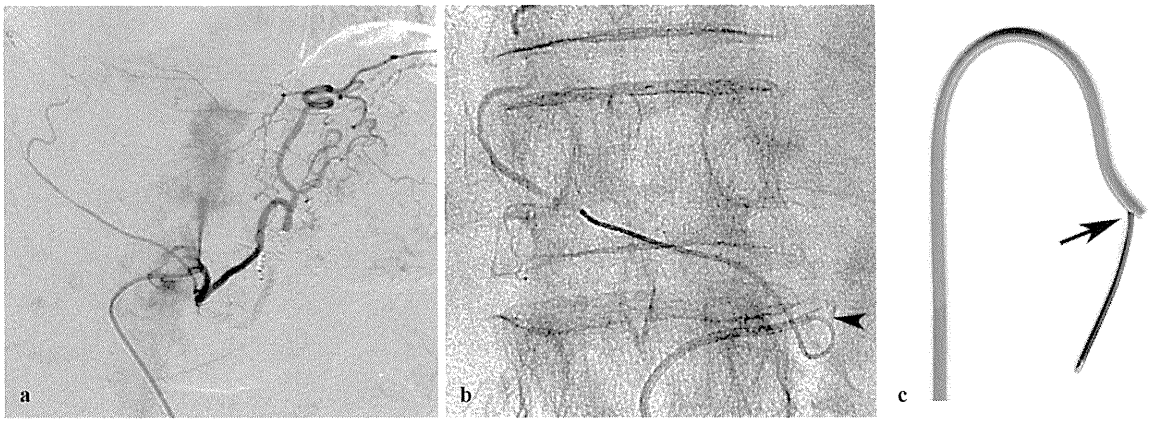


**Fig. 19.** **a** Common trunk of the bilateral IPAs turns downward, with an acute angle at the orifice. **b** Microcatheter is successfully introduced into the right IPA through the cleft at the caudal aspect (*arrowhead*). **c** Photograph of a cleft catheter and a microcatheter. *Arrow* indicates the cleft

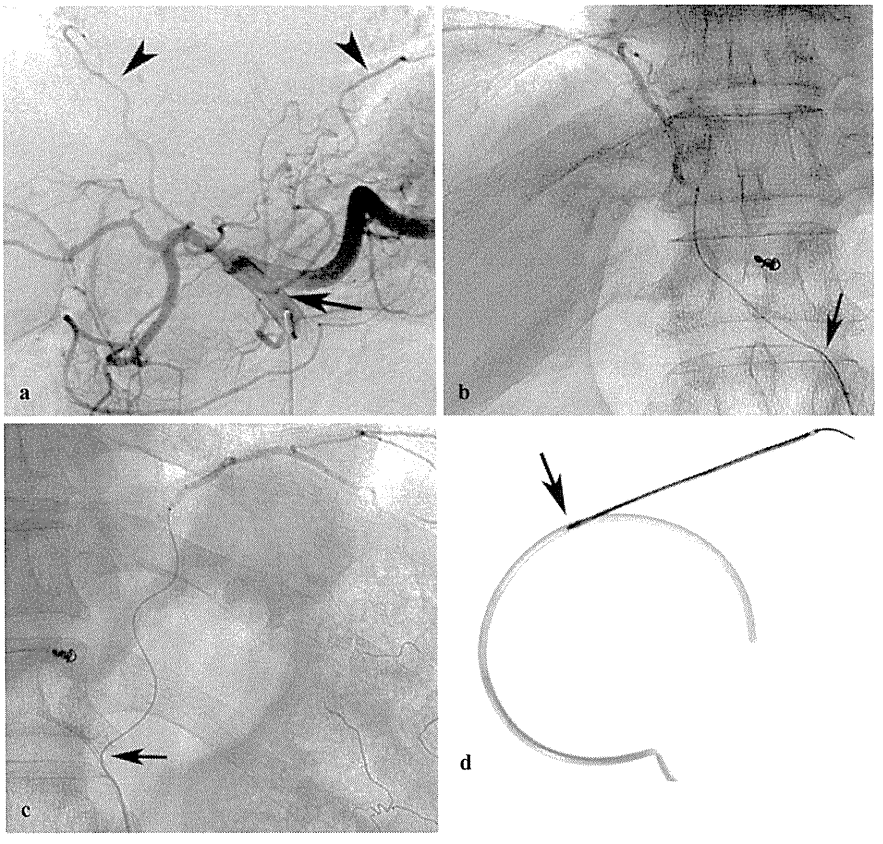


**Fig. 20.** **a** Celiac arteriogram shows the bilateral IPA (*arrowheads*) arising from the distal portion of the celiac trunk (*arrow*). **b** The microcatheter is successfully introduced into the right IPA through a large side hole of the catheter (*arrow*). **c** The left IPA is also selected successfully through the side hole (*arrow*). **d** Photograph of a catheter with a large side hole and a microcatheter. *Arrow* indicates the side hole

that used for TACE of the hepatic artery[4] (i.e., to almost half the dosage).

## Conclusion

The IPA, although a small vessel, is the most common extrahepatic collateral vessel supplying HCCs. Because in addition to the complexity of reconstructed pathways frequently the origin of the IPA and its branches varies, thorough knowledge of the vascular anatomy and variations of the IPA is critical to transcatheter management of HCCs. Several techniques may facilitate effective, safe TACE through an IPA that is difficult to select by the conventional coaxial technique; such techniques can reduce both the procedural time and the incidence of complications.

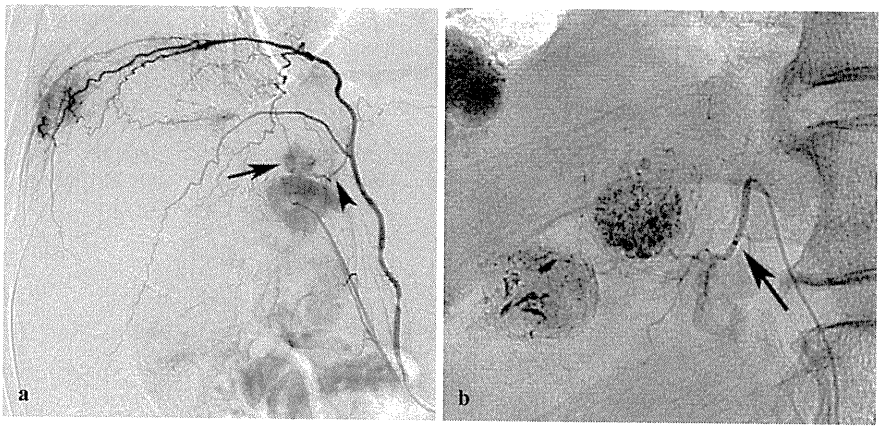


**Fig. 21.** **a** Arteriography of the right IPA arising from the right superior polar renal artery shows a tumor stain (*arrow*) supplied by a small branch derived from the anterior branch (*arrowhead*). Pleural and pulmonary staining and pulmonary vessel are also seen. **b** The small vessel was successfully selected, and TACE was performed. *Arrow* indicates the catheter tip

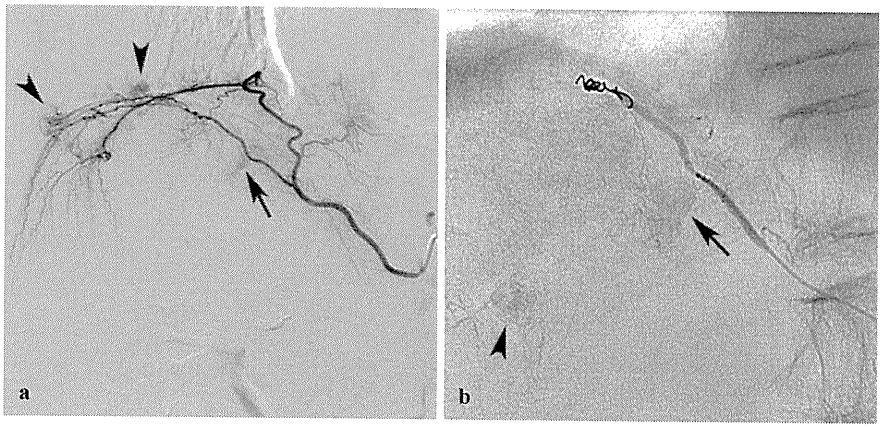


**Fig. 22.** **a** Arteriography of the right IPA shows a tumor stain (*arrow*) and pulmonary staining (*arrowheads*) from the posterior branch. **b** The tumor-feeding branch was small and could not be selected. TACE was performed after coil embolization of the posterior branch distal to the feeding branch. *Arrow* indicates iodized oil accumulation in the tumor. *Arrowhead* shows the tumor that was simultaneously embolized through the hepatic branch

## References


1. Loukas M, Hullett J, Wagner T. Clinical anatomy of the inferior phrenic artery. Clin Anat 2005;18:357–65.
2. Chung JW, Park JH, Han JK, Choi BI, Kim TK, Han MC. Transcatheter oily chemoembolization of the inferior phrenic artery in hepatocellular carcinoma: the safety and potential therapeutic role. J Vasc Interv Radiol 1998;9:495–500.
3. Kim HC, Chung JW, Lee W, Jae HJ, Park JH. Recognizing extrahepatic collateral vessels that supply hepatocellular carcinoma to avoid complications of transcatheter arterial chemoembolization. Radiographics 2005;25:S25–39.
4. Miyayama S, Matsui O, Taki K, Minami T, Ryu Y, Ito C, et al. Extrahepatic blood supply to hepatocellular carcinoma: angiographic demonstration and transcatheter arterial chemoembolization. Cardiovasc Intervent Radiol 2006;29:39–48.
5. Miyayama S, Yamashiro M, Okuda M, Yoshie Y, Nakashima Y, Ikeno H, et al. The march of extrahepatic collaterals: analysis of blood supply to hepatocellular carcinoma located in the bare area of the liver after chemoembolization. Cardiovasc Intervent Radiol 2010;33:513–22.
6. Gwon DI, Ko GY, Yoon HK, Sung KB, Lee JM, Ryu SJ, et al. Inferior phrenic artery: anatomy, variations, pathologic conditions, and interventional management. Radiographics 2007;27:687–705.
7. Hieda M, Toyota N, Kakizawa H, Ishikawa M, Horiguchi J, Ito K. The anterior branch of the left inferior phrenic artery arising from the right inferior phrenic artery: an angiographic and CT study. Cardiovasc Intervent Radiol 2009;32:250–4.
8. Miyayama S, Matsui O, Akakura Y, Yamamoto T, Fujinaga Y, Koda W, et al. Use of a catheter with a large side hole for selective catheterization of the inferior phrenic artery. J Vasc Interv Radiol 2001;12:497–9.
9. Kiyosue H, Matsumoto S, Hori Y, Okahara M, Sagara Y, Mori H. Turn-back technique with use of a shaped microcatheter for superselective catheterization of arteries originating at acute angle. J Vasc Interv Radiol 2004;15:641–3.
10. Miyayama S, Yamashiro Y, Okuda M, Aburano H, Shigenari N, Morinaga K, et al. Creation of a cleft in an angiography catheter to facilitate catheterization of branches of the aorta arising at an acute angle. J Vasc Interv Radiol 2008;19:1769–71.
11. So YH, Chung JW, Yin YH, Jae HJ, Jeon UB, Cho BH, et al. The right inferior phrenic artery: origin and proximal anatomy on digital subtraction angiography and thin-section helical computed tomography. J Vasc Interv Radiol 2009;20:1164–71.
12. Lee IJ, Chung JW, Kim HC, Yin YH, So YH, Jeon UB, et al. Extrahepatic collateral artery supply to the tumor thrombi of hepatocellular carcinoma invading inferior vena cava: the prevalence and determinant factors. J Vasc Interv Radiol 2009;20:22–9.
13. Netter FH. The Ciba collection of medical illustrations. Digestive system. Part II. Lower digestive tract. New York: Ciba-Geigy; 1962. p. 35–6.

14. Miyayama S, Matsui O, Taki K, Minami T, Ito C, Shinmura R, et al. Transcatheter arterial chemoembolization for hepatocellular carcinoma fed by the reconstructed inferior phrenic artery: anatomical and technical analysis. J Vasc Interv Radiol 2004;15:815–23.
15. Matsumoto K, Nojiri J, Takase Y, Egashira Y, Azama S, Kato A, et al. Cerebral Lipiodol embolism: a complication of transcatheter arterial chemoembolization for hepatocellular carcinoma. Cardiovasc Intervent Radiol 2007;30:512–4.
16. Miyayama S, Yamashiro M, Okuda M, Aburano H, Shigenari N, Morinaga K, et al. Anastomosis between the hepatic artery and the extrahepatic collateral or between extrahepatic collaterals: observation on angiography. J Med Imag Radiat Oncol 2009;53:271–82.

Jpn J Radiol (2010) 28:555–562
DOI 10.1007/s11604-010-0471-8

PICTORIAL ESSAY

# Hepatocellular carcinoma in the caudate lobe of the liver: variations of its feeding branches on arteriography

**Shiro Miyayama · Masashi Yamashiro · Yuichi Yoshie**
**Yoshiko Nakashima · Hiroshi Ikeno · Nobuaki Orito**
**Miki Yoshida · Osamu Matsui**

Received: March 26, 2010 / Accepted: May 27, 2010


**Abstract** There are usually multiple caudate arteries arising from the right, left, and middle hepatic arteries, and they are frequently connected to each other. Therefore, hepatocellular carcinoma (HCC) in the caudate lobe is frequently fed by multiple branches arising from different origins. HCC located in the Spiegel lobe is usually fed by the caudate arteries derived from the right and/or left hepatic artery. HCC in the paracaval portion is mainly fed by the caudate artery derived from the right hepatic artery; with low frequency, it is fed by the caudate artery derived from the left hepatic artery. HCC in the caudate process is usually fed by the caudate artery derived from the right hepatic artery. Because of the complexity and overlap of vascular territories, the tumor-feeding branch of a recurrent HCC lesion in the caudate lobe frequently changes on follow-up arteriograms. In addition, several extrahepatic collateral vessels supply the recurrent tumor. To perform effective transcatheter arterial chemoembolization (TACE) for HCC in the caudate lobe, radiologists should have sufficient knowledge of vascular anatomy supplying HCC in the caudate lobe.

**Key words** Hepatocellular carcinoma · Caudate lobe · Vascular anatomy · Chemoembolization

S. Miyayama (✉) · M. Yamashiro · Y. Yoshie · Y. Nakashima · H. Ikeno, N. Orito · M. Yoshida
Department of Diagnostic Radiology, Fukuiken Saiseikai Hospital, 7-1 Funabashi, Wadanaka-cho, Fukui 918-8503, Japan
Tel. +81-776-23-1111; Fax +81-776-28-8519
e-mail: s-miyayama@fukui.saiseikai.or.jp

O. Matsui
Department of Radiology, Kanazawa University Graduate School of Medical Science, Kanazawa, Japan

## Introduction

The caudate lobe is centrally located in the liver, between the right and left lobes. Because of this anatomical location, hepatocellular carcinoma (HCC) arising in the caudate lobe is difficult to treat. Surgical resection of the caudate lobe has a high mortality rate, in addition to a high recurrence rate of the tumor.[1,2] Percutaneous ablation therapy (e.g., radiofrequency ablation) is a useful alternative treatment,[3,4] but the procedure might be technically difficult because of the deep tumor location and adjacent large vessels. Therefore, transcatheter arterial chemoembolization (TACE) plays an important role in the treatment of HCC in the caudate lobe.[5,6]

Because there are usually multiple caudate arteries arising from the right, left, and middle hepatic arteries, HCC in the caudate lobe is frequently fed by multiple branches arising from different origins.[5–9] In addition, the feeding branches become more complex when the tumor recurs after TACE. These factors might make it more difficult to control HCC in the caudate lobe by TACE. To perform effective TACE for HCC in the caudate lobe, radiologists should have sufficient knowledge of vascular anatomy supplying HCC in the caudate lobe.

## Subsegments of the caudate lobe

The caudate lobe is divided into three subsegments according to portal vein ramification: Spiegel lobe, paracaval portion, caudate process. The Spiegel lobe is the protuberant hepatic portion to the left of the intrahepatic vena cava.[10] The paracaval portion is in front of the intrahepatic vena cava and is surrounded by the right

and middle hepatic veins.[10,11] The caudate process is a tongue-like projection between the vena cava and adjacent portal vein.[10] Theoretically, there are multiple caudate arteries supplying these three subsegments.

## Caudate artery anatomy

A cadaver dissection study by Mizumoto and Suzuki[7] reported that the caudate arteries arose from the posterior segmental artery of the right hepatic artery and left hepatic artery in 32.1%, from the posterior segmental artery of the right hepatic artery and middle hepatic artery in 26.4%, and from the three arteries in 20.8%. However, in a previous angiographic observation, the incidences of the caudate artery derived from the left hepatic artery and the posterior segmental artery of the right hepatic artery were low. Because the left hepatic lobe has limited depth, identification of the caudate artery is difficult even on stereoarteriograms.[9] In addition, the caudate artery derived from the posterior segmental artery is frequently difficult to recognize because it mimics the posterior segmental artery of the right hepatic artery.[9]

With advances in digital subtraction angiography systems and catheter technology, two or more caudate arteries arising from the right hepatic, middle hepatic, and/or left hepatic artery can be demonstrated in almost all cases. In the right hepatic artery, the caudate artery arises between the proximal portion of the right hepatic artery and the main trunk of the anterior or posterior segmental artery of the right hepatic artery (Figs. 1–7). On the left side, the caudate artery usually arises between the proximal portion and umbilical portion of the left hepatic artery (Figs. 3, 8). The caudate artery also arises from the proximal portion of the middle hepatic artery or medial segmental artery (Fig. 9). It infrequently arises with the cystic artery as a common trunk (Fig. 10). Additionally, it infrequently arises from the proper hepatic (Fig. 11), common hepatic, or extrahepatic artery (Fig. 12).

Among the caudate arteries derived from the right hepatic artery, the paracaval branch runs upwardly (Fig. 4), and the Spiegel lobe branch runs to the left (Figs. 1–5, 11). These branches frequently arise as a common trunk (Figs. 4, 13). Selective arteriography of the Spiegel lobe branch shows a typical hepatogram indicating the contour of the Spiegel lobe (Figs. 1, 9, 11, 13). The caudate process branch usually mimics the posterior segmental artery of the right hepatic artery (Fig. 13). Among the caudate arteries derived from the left hepatic artery, the Spiegel lobe branch usually mimics the lateral segmental artery (Fig. 3), and the paracaval branch mimics the medial segmental artery (Figs. 9, 13).

The caudate arteries are frequently connected to each other as well as to the medial segmental artery (Fig. 7).[12–14]

## Hepatocellular carcinoma

### HCC in the Spiegel lobe

HCC located in the Spiegel lobe is usually fed by the caudate arteries derived from the right and/or left hepatic artery.[5,6] Almost all feeding branches mainly arise from the proximal portion of the right and left hepatic artery (Figs. 1–3). In addition, the caudate artery arising from the proximal portion of the middle hepatic or medial segmental artery supplies tumors in the Spiegel lobe (Fig. 9). Because the Spiegel lobe protrudes from the liver, a large tumor is frequently found to be fed by extrahepatic collateral vessels at the initial discovery.

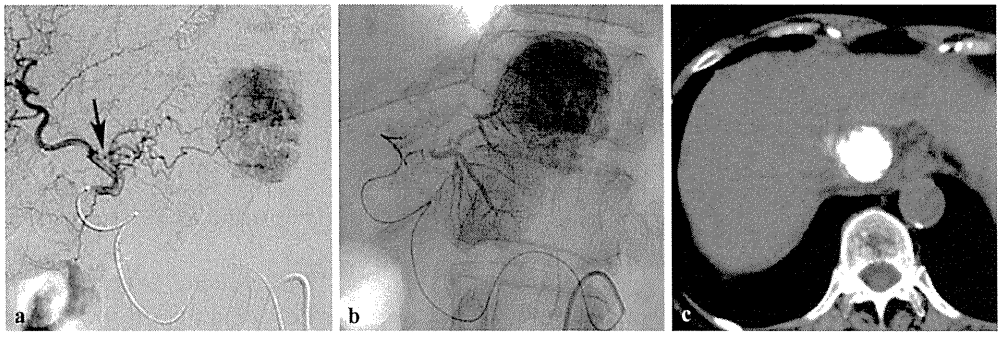


**Fig. 1.** Hepatocellular carcinoma (HCC) in the Spiegel lobe. **a** Arteriogram of the right hepatic artery shows a tumor stain in the Spiegel lobe supplied by the caudate artery derived from the right hepatic artery (*arrow*). **b** The caudate artery was selected, and transcatheter arterial chemoembolization (TACE) was performed. The contour of the Spiegel lobe is clearly seen. **c** Computer tomography (CT) 1 week after TACE shows dense iodized oil accumulation in the tumor

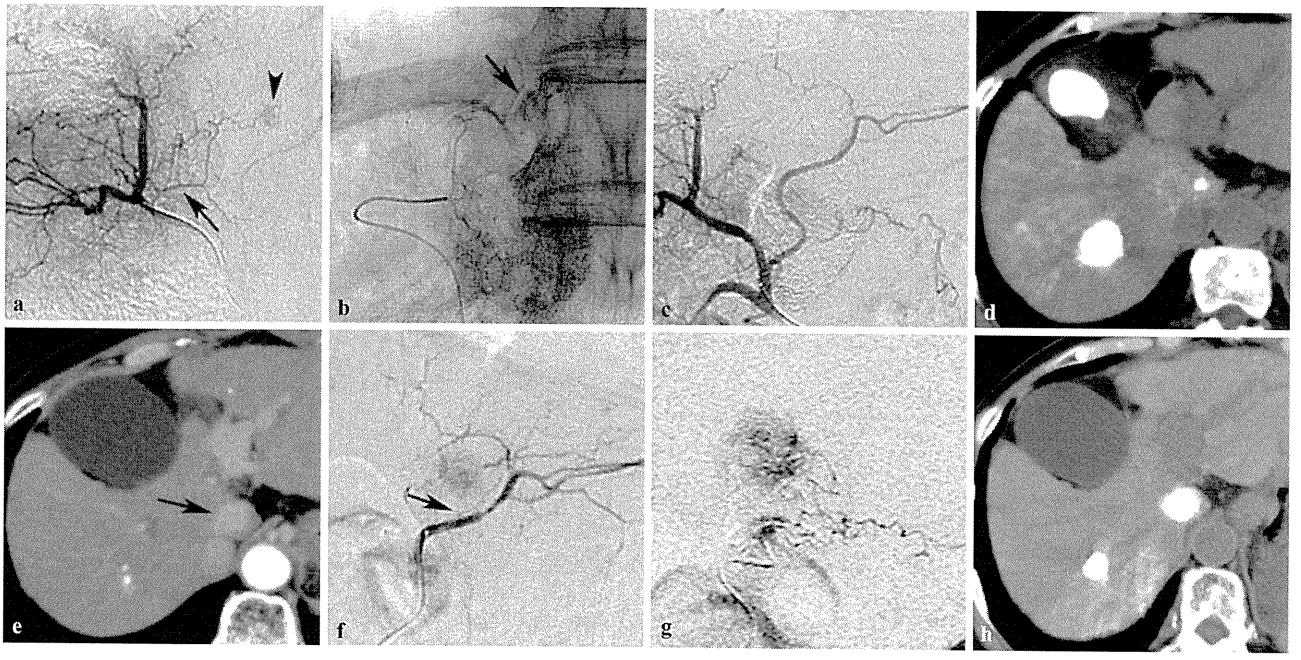

**Fig. 2.** HCC in the Spiegel lobe. **a** Arteriogram of the right hepatic artery obtained after TACE of the anterosuperior subsegmental artery of the right hepatic artery shows a tumor stain (*arrowhead*) supplied by the caudate artery derived from the anterior segmental artery of the right hepatic artery (*arrow*). **b** The caudate artery was selected, and TACE was performed. The contour of the Spiegel lobe was clearly seen. *Arrow* points to the tumor. **c** Proper hepatic arteriogram obtained immediately after TACE shows no residual tumor stain. **d** CT 1 week after TACE shows dense iodized oil accumulation in both tumors. **e** Arterial phase CT 3 years after TACE shows a recurrent tumor in the Spiegel lobe (*arrow*). **f** Follow-up arteriogram shows a tumor stain supplied by the caudate artery derived from the left hepatic artery (*arrow*) that was not seen in **c**. **g** The branch was selected, and TACE was performed. **h** CT 1 week after additional TACE shows dense iodized oil accumulation in the tumor

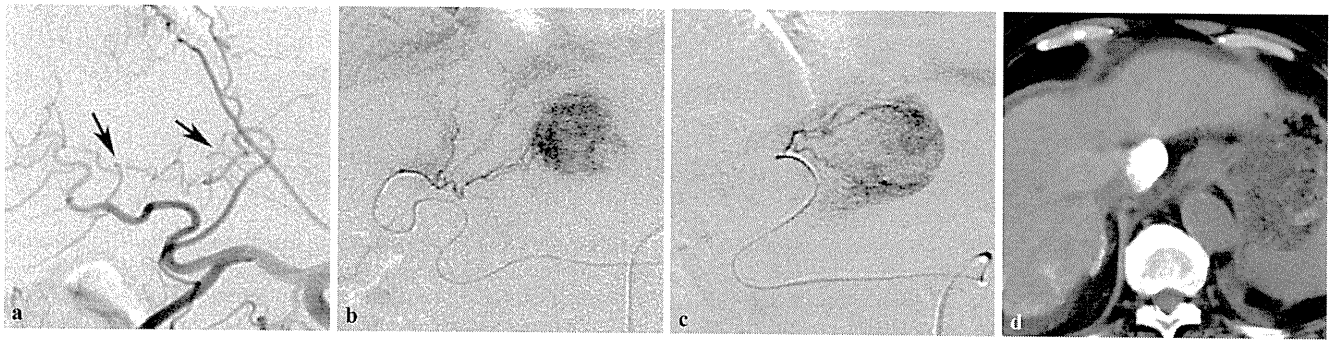

**Fig. 3.** HCC in the Spiegel lobe. **a** Celiac arteriogram shows two caudate arteries derived from the right and left hepatic artery, respectively (*arrows*). **b** First, the caudate artery derived from the right hepatic artery was selected, and TACE was performed. **c** Second, the caudate artery derived from the left hepatic artery was selected, and TACE was performed. **d** CT 1 week after TACE shows dense iodized oil accumulation in the tumor. Iodized oil was also accumulated in the right adrenal gland because the right inferior phrenic artery was subsequently embolized to treat another tumor (not shown)

## HCC in the paracaval portion

When HCC is in the paracaval portion, it is mainly fed by the caudate artery derived from the right hepatic artery.[5,6] Several feeding branches frequently arise between the right hepatic artery and the proximal portion of the anterior or posterior segmental artery of the right hepatic artery (Fig. 6). Another feeding branch also arises from the left hepatic artery (Fig. 13). The tumor in the paracaval portion is rarely supplied by the caudate artery derived from the left hepatic artery alone (Fig. 8).

## HCC in the caudate process

HCC in the caudate process is usually fed by the caudate artery derived from the right hepatic artery (Fig. 4).[5,6]

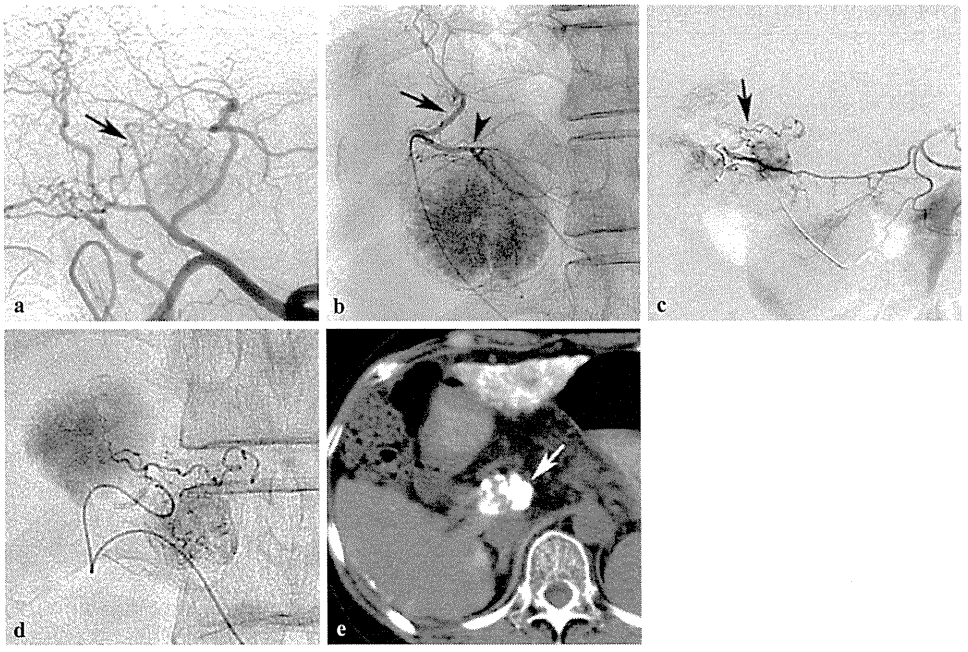


**Fig. 4.** HCC in the caudate process. **a** Celiac arteriogram shows a tumor stain supplied by the hypertrophied caudate artery derived from the right hepatic artery (*arrow*). **b** Spot radiograph obtained during TACE showed that the Spiegel branch (*arrowhead*) and paracaval branch (*arrow*) arose as a common trunk. **c** Two years later, a new lesion developed near the previous tumor site. Arteriogram of the right gastric artery shows a tumor stain supplied by a small branch (*arrow*). **d** The branch was selected, and TACE was performed. **e** CT 1 week after TACE shows dense iodized oil accumulation in the tumor (*arrow*). Iodized oil was also seen in the left lobe of the liver because the left hepatic artery was subsequently embolized to treat other tumors (not shown)

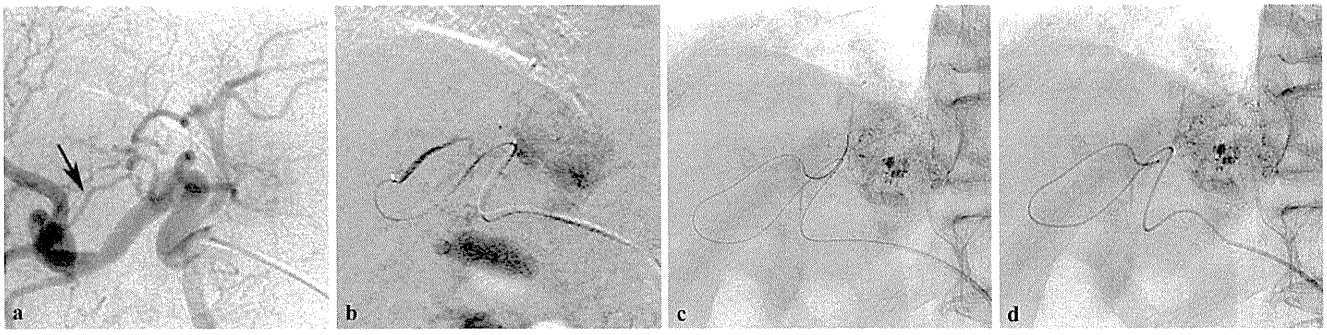


**Fig. 5.** HCC in the Spiegel lobe. **a** Celiac arteriogram shows a tumor stain supplied by the right hepatic artery (*arrow*). **b** The caudate artery was selected using a shaped microcatheter. The guidewire was advanced into the caudate artery, but the microcatheter could not be advanced into it. **c** The shaped microcatheter was withdrawn and exchanged for a thinner flexible microcatheter. **d** The microcatheter was deeply advanced into the caudate artery using an over-the-wire technique, and TACE was completed

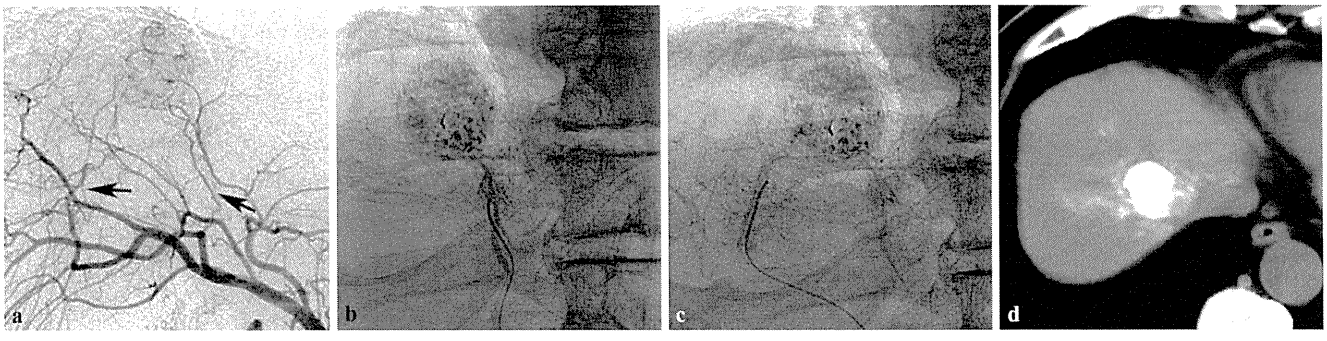


**Fig. 6.** HCC in the paracaval portion. **a** Common hepatic arteriogram shows a tumor stain supplied by two caudate arteries derived from different sites (*arrows*). **b** First, the caudate artery derived from the anterior segmental artery of the right hepatic artery was selected and TACE was performed. **c** Second, the caudate artery derived from another anterior segmental artery of the right hepatic artery was selected, and TACE was performed. **d** CT 1 week after TACE shows dense iodized oil accumulation in the tumor

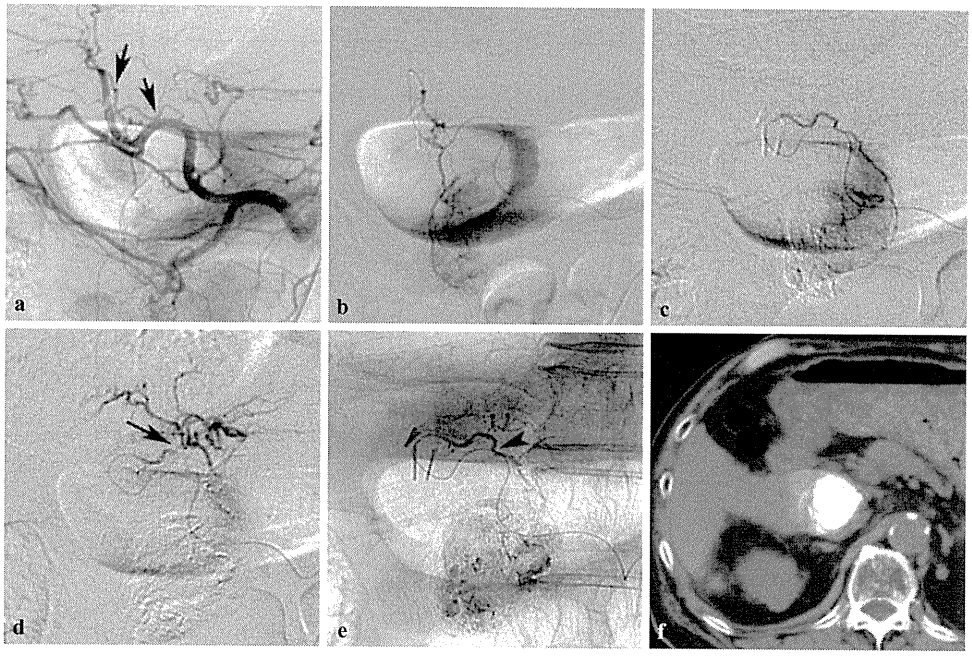

**Fig. 7.** HCC in the Spiegel lobe. **a** Celiac arteriogram shows two caudate arteries derived from the anterior segmental artery of the right hepatic artery (*arrows*). **b** First, one of the caudate arteries was selected, and TACE was performed. **c** Second, another caudate artery was selected, and TACE was started. **d** Arteriogram obtained during TACE shows the left hepatic artery through the anastomosis (*arrow*). **e** Then, the microcatheter was advanced distally to the anastomosed branch, and TACE was completed. **f** CT 1 week after TACE shows dense iodized oil accumulation in the tumor

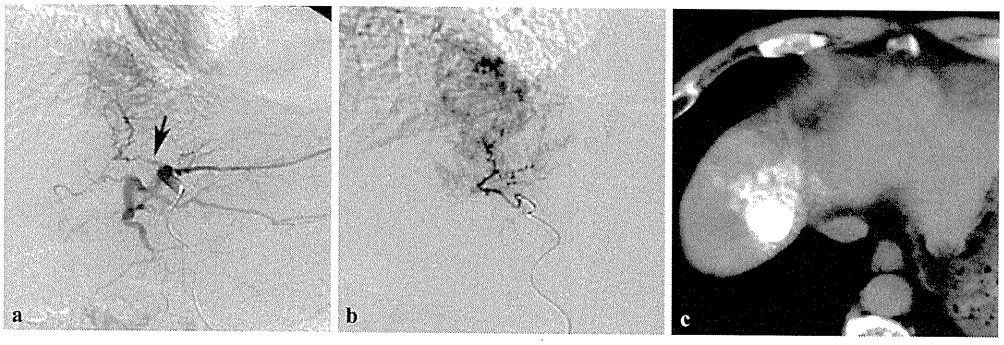

**Fig. 8.** HCC in the paracaval portion. **a** Arteriogram of the left hepatic artery shows a tumor stain supplied by the caudate artery derived near the umbilical portion of the left hepatic artery (*arrow*). **b** The vessel was selected, and TACE was performed. **c** CT 1 week after TACE shows dense iodized oil accumulation in the tumor

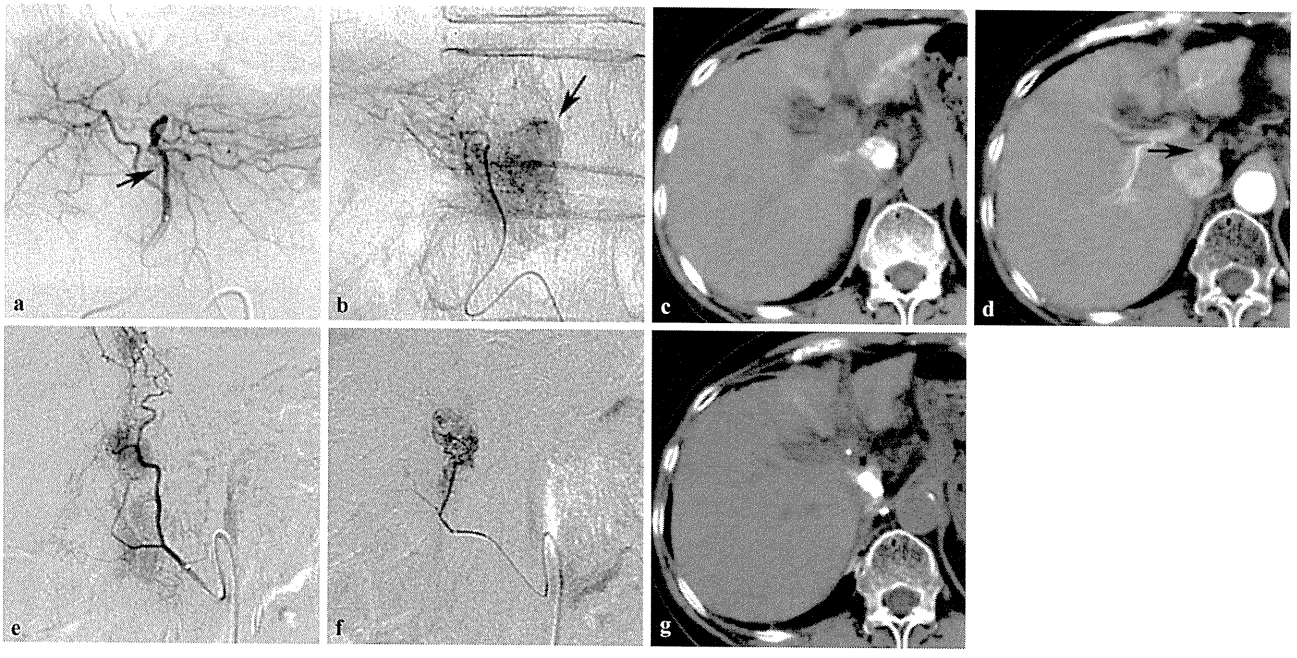

**Fig. 9.** HCC in the Spiegel lobe. **a** Arteriogram of the left hepatic artery shows the caudate artery derived from the medial segmental artery (*arrow*). **b** The vessel was selected, and TACE was performed. The contour of the Spiegel lobe was seen. *Arrow* points to the tumor. **c** CT 1 week after TACE shows dense iodized oil accumulation in the tumor. **d** However, CT 13 months after TACE shows a recurrent tumor (*arrow*). **e** On additional angiography, the previously embolized caudate artery was occluded (not shown). The tumor was supplied by the right inferior phrenic artery alone. **f** The tumor-feeding branch was selected, and TACE was performed. **g** CT 1 week after TACE shows dense iodized oil accumulation in the tumor

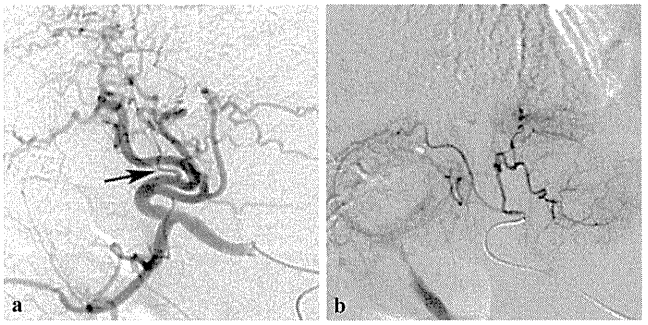

**Fig. 10.** Caudate artery derived from the cystic artery. **a** Common hepatic arteriogram shows that the cystic artery derived from the proximal portion of the right hepatic artery (*arrow*). **b** Selective arteriogram shows that the caudate artery was derived from the cystic artery

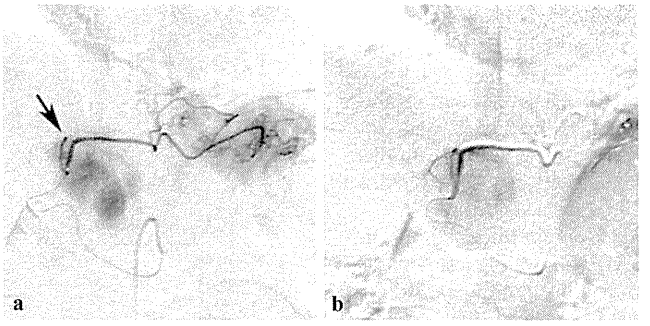

**Fig. 12.** HCC in the Spiegel lobe. **a** Arteriogram of the accessory left gastric artery shows a tumor stain supplied by a small branch (*arrow*). **b** The branch could not be directly selected; therefore, TACE was performed after embolization of the accessory left gastric artery using metallic coils and *n*-butyl-cyanoacrylate

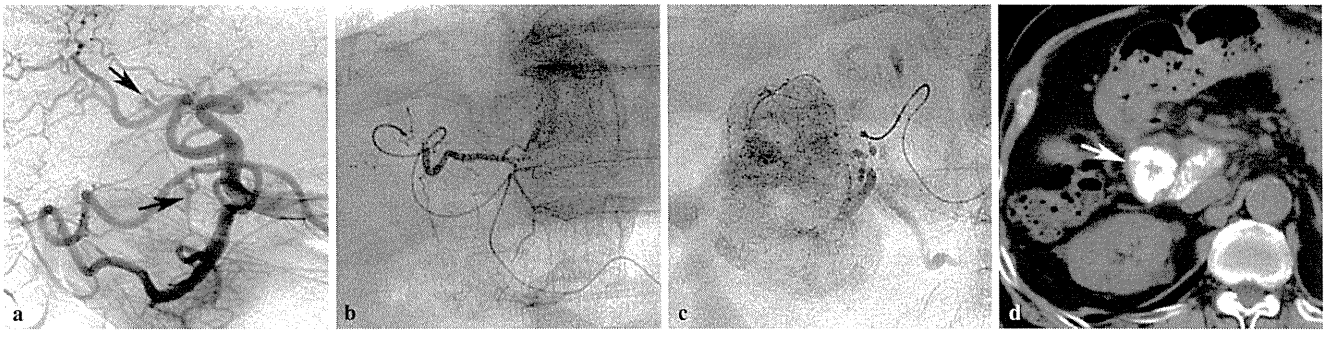

**Fig. 11.** HCC in the caudate process. **a** Common hepatic arteriogram shows two caudate arteries (*arrow*). **b** First, the Spiegel lobe branch derived from the right hepatic artery was selected, and TACE was performed. The contour of the Spiegel lobe is clearly seen. **c** Second, the caudate process branch derived from the proper hepatic artery was selected, and TACE was performed. This vessel was a main feeder of the tumor. **d** CT 1 week after TACE shows dense iodized oil accumulation in the tumor (*arrow*)

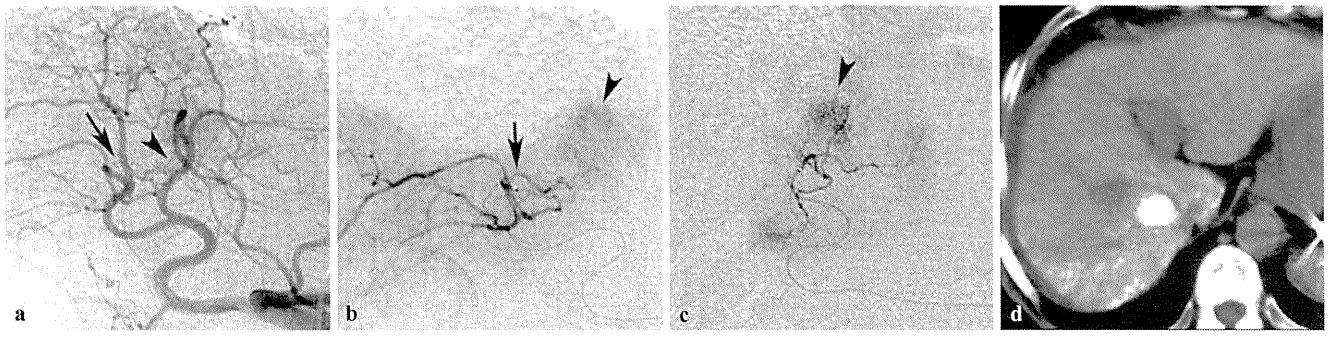

**Fig. 13.** HCC in the paracaval portion. **a** Celiac arteriogram shows two caudate arteries derived from the left hepatic artery (*arrowhead*) and the posterior segmental artery of the right hepatic artery (*arrow*). **b** Arteriogram of the posterior segmental artery of the right hepatic artery shows a tumor stain (*arrowhead*). *Arrow* indicates the caudate artery. **c** Arteriogram of the caudate artery derived from the left hepatic artery also shows the tumor stain (*arrowhead*). **d** CT 1 week after TACE shows dense iodized oil accumulation in the tumor

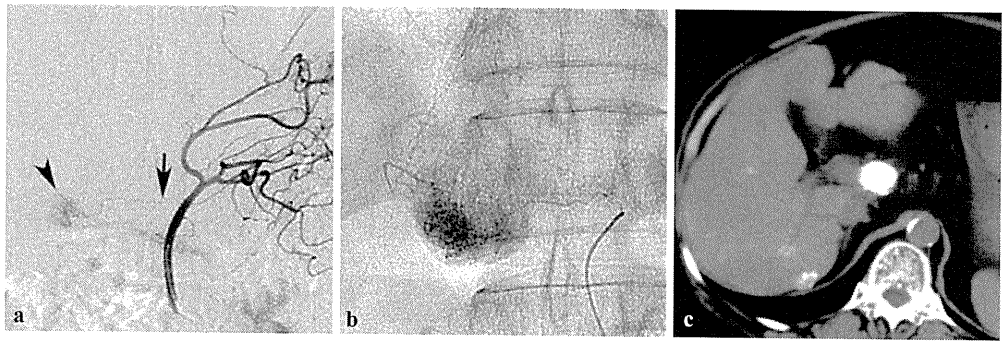


**Fig. 14.** Recurrent HCC in the Spiegel lobe. **a** Arteriogram of the left gastric artery shows a tumor (*arrowhead*) supplied by a small branch (*arrow*). **b** The branch was selected, and TACE was performed. **c** CT 1 week after TACE shows dense iodized oil accumulation in the tumor

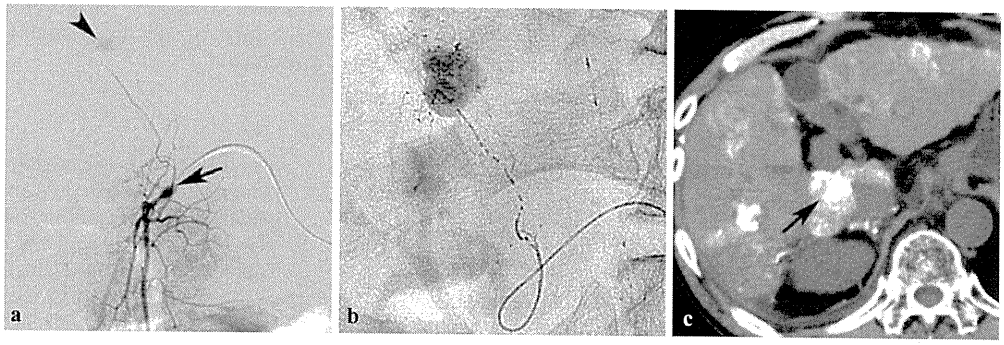


**Fig. 15.** Recurrent HCC in the caudate process. **a** Arteriogram of the posterosuperior pancreatoduodenal artery shows a small tumor stain (*arrowhead*) supplied by the 3 o'clock and 9 o'clock arteries (*arrow*). **b** The vessel was selected, and TACE was performed. **c** CT 1 week after TACE shows dense iodized oil accumulation in the tumor (*arrow*)

The caudate artery derived from the proper hepatic artery also supplies tumors in the caudate process (Fig. 11).

### Changes in tumor-feeding branches of recurrent tumors

Because of the presence of multiple caudate arteries and the overlap of these vascular territories, the tumor-feeding branch of a recurrent tumor in the caudate lobe frequently changes on follow-up arteriograms.[6] Another caudate artery arising from a different origin replaces the tumor-feeding branch; in particular, a small feeding branch becomes sufficiently hypertrophied to be detected on angiography (Fig. 2).

Extrahepatic arteries frequently supply the recurrent tumor in the caudate lobe, particularly the tumor in the Spiegel lobe. The right inferior phrenic (Fig. 9), right or left gastric (Figs. 4, 14), dorsal pancreatic, right adrenal, and right renal capsular arteries are possible collateral vessels for recurrent tumors in the Spiegel lobe. The 3 o'clock and 9 o'clock arteries are also possible collateral vessels for recurrent tumors in the caudate process (Fig. 15). In addition, recurrent HCC in the paracaval portion is supplied by the right inferior phrenic artery.

### Catheterization technique in the caudate artery

Owing to proximal branching of the caudate artery, non-selective TACE is not effective for HCC in the caudate lobe.[8,9] Because the caudate artery usually has a small caliber, a microcatheter with a tip less than 2F facilitates selective catheterization. As the caudate artery frequently arises at an acute angle, shaping the microcatheter by steam-heating is useful for selective catheterization. When the tip of the microcatheter faces the orifice of the caudate artery, a guidewire is inserted into the caudate artery, and the microcatheter is then advanced into the branch. An over-the-wire technique to exchange the shaped microcatheter for a flexible one is also useful if the shaped microcatheter cannot be advanced into the caudate artery (Fig. 5). For arterial blockage distal to the caudate artery, use of a microballoon catheter has been reported.[15] In a small branch derived from extrahepatic collateral pathways, embolization using a metallic coil and/or *n*-butyl-cyanoacrylate at the distal portion of the small feeding branch is also useful when it cannot be directly selected (Fig. 12).

Multiple caudate arteries frequently anastomose to each other to form an arcade.[12–14] When the embolic materials are injected from one of the caudate arteries,

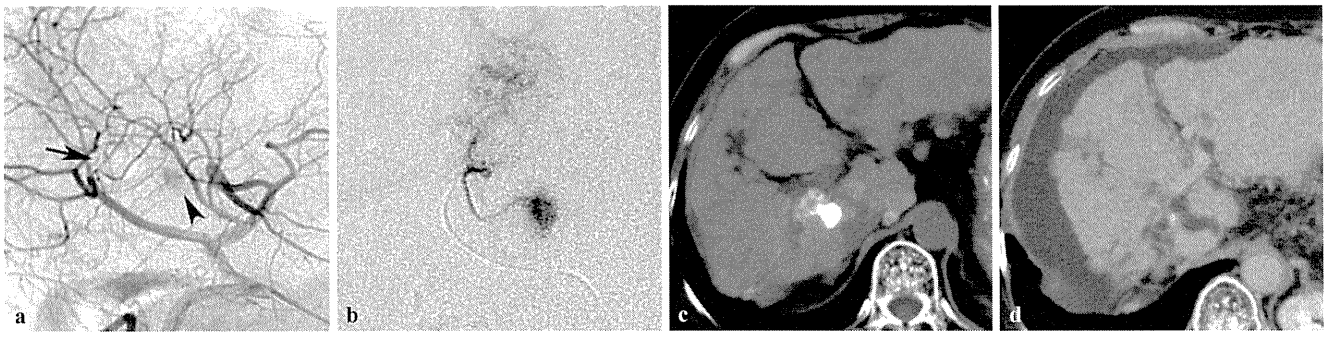

**Fig. 16.** Bile duct dilatation after TACE of the caudate artery. **a** Common hepatic arteriogram shows a small tumor stain (*arrowhead*) supplied by the caudate artery derived from the anterior segmental artery of the right hepatic artery (*arrow*). **b** The caudate artery was selected, and TACE was performed. **c** CT 1 week after TACE shows dense iodized oil accumulation in the tumor. **d** CT 6 years after TACE shows that the tumor was well controlled. However, the bile duct was dilated in the right lobe of the liver, and the right lobe of the liver was atrophied

collateral blood flow through the other caudate arteries reverses the blood flow in the embolized artery and pushes back the embolic materials.[5,9] If possible, the microcatheter should be advanced distal to the anastomosis branch to avoid inadvertent widespread embolization (Fig. 7). Small branches supplying the main bile duct usually arise from the caudate artery[12]; therefore, bile duct stricture may occur after TACE of the caudate artery (Fig. 16).[14] This is a rare but serious complication of TACE through the caudate artery.

## Conclusion

The caudate artery usually arises from the proximal portion of the hepatic artery. The vascular supply to HCC in the caudate lobe is complex because of the presence of multiple caudate arteries and their overlapped vascular territories. In addition, several extrahepatic collateral vessels feed recurrent tumors in the caudate lobe. Identification of the tumor-feeding caudate artery and selective catheterization is essential to perform effective TACE.

## References


1. Tanaka S, Shimada M, Shirabe K, Maehara S, Tsujita E, Taketomi A, et al. Surgical outcome of patients with hepatocellular carcinoma originating in the caudate lobe. Am J Surg 2005;190:451–5.
2. Shimada M, Matsumata T, Maeda T, Yanaga K, Taketomi A, Sugimachi K. Characteristics of hepatocellular carcinoma originating in the caudate lobe. Hepatology 1994;19:911–5.
3. Shibata T, Maetani Y, Ametani F, Kubo T, Itoh K, Konishi J. Efficacy of nonsurgical treatments for hepatocellular carcinoma in the caudate lobe. Cardiovasc Intervent Radiol 2002;25:186–92.
4. Yamakado K, Nakatsuka A, Akeboshi M, Takaki H, Takeda K. Percutaneous radiofrequency ablation for the treatment of liver neoplasms in the caudate lobe left of the vena cava: electrode placement through the left lobe of the liver under CT-fluoroscopic guidance. Cardiovasc Intervent Radiol 2005;28:638–40.
5. Terayama N, Miyayama S, Tatsu H, Yamamoto T, Toya D, Tanaka N, et al. Subsegmental transcatheter arterial embolization for hepatocellular carcinoma in the caudate lobe. J Vasc Interv Radiol 1998;9:501–8.
6. Yoon CJ, Chung JW, Cho BH, Jae HJ, Kang SG, Kim HC, et al. Hepatocellular carcinoma in the caudate lobe of the liver: angiographic analysis of tumor-feeding arteries according to subsegmental location. J Vasc Intev Radiol 2008;19:1543–50.
7. Mizumoto R, Suzuki H. Surgical anatomy of the hepatic hilum with special reference to the caudate lobe. World J Surg 1998;12:2–10.
8. Takayasu K, Muramatsu Y, Shima Y, Goto H, Moriyama N, Yamada T, et al. Clinical and radiologic features of hepatocellular carcinoma originating in the caudate lobe. Cancer 1986;58:1557–62.
9. Miyayama S, Matsui O, Kameyama T, Hirose J, Konishi H, Choto S, et al. Angiographic anatomy of arterial branches to the caudate lobe of the liver; with special reference to its effect on transarterial embolization for hepatocellular carcinoma. Jpn J Clin Radiol 1990;35:353–9 (in Japanese).
10. Kumon M. Anatomy of the caudate lobe with special reference to portal vein and bile duct. Acta Hepatol Jpn 1985;26:1193–9 (in Japanese).
11. Matsui O, Takashima T, Kadoya M, Hirose J, Kameyama T, Choto S, et al. CT anatomy of para-caval portion of the caudate lobe of the liver. Nippon Igaku Hoshasen Gakkai Zasshi 1988;48:841–6 (in Japanese).
12. Stapleton GN, Hickman R, Terblanche J. Blood supply of the right and left hepatic ducts. Br J Surg 1998;85:202–7.
13. Miyayama S, Matsui O, Taki K, Minami T, Ryu Y, Ito C, et al. Arterial blood supply to the posterior aspect of segment IV of the liver from the caudate branch: demonstration at CT after iodized oil injection. Radiology 2005;237:1110–4.
14. Miyayama S, Yamashiro M, Okuda M, Yoshie Y, Nakashima Y, Ikeno H, et al. Main bile duct stricture occurring after transcatheter chemoembolization for hepatocellular carcinoma. Cardiovasc Intervent Radiol 2010 Jan 8. [Epub ahead of print].
15. Ishimaru H, Ishimaru K, Mitarai K, Koshiishi T, Matsuoka Y, Egawa A, et al. Application of coaxial micro-balloon catheter (Attendant) for treatment of hepatocellular carcinoma. Jpn J Intervent Radiol 2007;22:72–5 (in Japanese).

# Chemoembolization for the Treatment of Large Hepatocellular Carcinoma

Shiro Miyayama, MD, Masashi Yamashiro, MD, Miho Okuda, MD, Yuichi Yoshie, MD, Natsuki Sugimori, MD, Saya Igarashi, MD, Yoshiko Nakashima, MD, Kazuo Notsumata, MD, Daisyu Toya, MD, Nobuyoshi Tanaka, MD, Takeshi Mitsui, MD, and Osamu Matsui, MD

**PURPOSE:** To retrospectively evaluate the efficacy of chemoembolization for inoperable hepatocellular carcinoma (HCC) tumors larger than 5 cm in diameter.

**MATERIALS AND METHODS:** Chemoembolization was performed in 30 patients with HCCs with a largest diameter of more than 5 cm with three or fewer lesions and no portal vein tumor thrombus. The mean maximum tumor diameter was 7.7 cm ± 2.4. When the tumor was extremely large and had multiple feeding arteries, stepwise chemoembolization sessions at intervals of 3–10 weeks were performed. In addition, extrahepatic collateral supply was identified and embolized. Local therapeutic effects, survival rates, and complications were analyzed.

**RESULTS:** The mean follow-up period was 33.8 months ± 24.1. One to 13 chemoembolization sessions (mean, 4.0 sessions ± 3.0) were performed in each patient. Additionally, 62 collateral vessels were embolized in 21 patients, including 22 vessels in 14 patients at the initial procedure. Early tumor response rate 2–3 months after treatment was 43.3% by Response Evaluation Criteria In Solid Tumors. Complete radiologic response was achieved in 19 patients. Eleven patients died between 4 and 61 months after treatment (mean, 27.2 months ± 21.8), including four deaths unrelated to hepatic causes. Nineteen patients have survived for 6–103 months (mean, 37.5 months ± 25.2). Overall and progression free-survival rates at 1, 3, and 6 years were 82.3% and 66.0%, 73.9% and 57.6%, and 32.9% and 34.2%, respectively. Three infectious complications developed and were managed by interventions.

**CONCLUSIONS:** Chemoembolization was effective for large HCCs, although there is a risk of infectious complications after the procedure.

J Vasc Interv Radiol 2010; 21:1226–1234

Abbreviations: HCC = hepatocellular carcinoma, IPA = inferior phrenic artery, RF = radiofrequency

WITH advances in imaging modalities and screening of high-risk groups, it has become possible to detect small hepatocellular carcinoma (HCC). However, HCC may still be discovered in advanced stages because its clinical symptoms are infrequent. Surgical resection has been considered the most effective therapy for HCC tumors larger than 5 cm in diameter (ie, "large HCC"). However, only 41% of patients with HCC are candidates for hepatectomy in Japan because of the associated liver cirrhosis and occasional multicentricity (1). Liver transplantation is another surgical treatment option (2), but it is performed in a limited number of patients because of the lack of donors and high costs.

Recently, local therapeutic options, such as radiofrequency (RF) ablation, have been developed and play an important role in the treatment of unresectable HCC (3–5). However, the local control of tumors 3–5 cm in diameter (ie, "medium-sized HCC") by RF ablation is usually limited because of the limited area of coagulation necrosis compared with that for HCCs smaller than 3 cm in diameter (ie, "small HCC") (4,5). Additionally, RF ablation is typically contraindicated for large HCCs because of the difficulty in completely ablating such tumors (4).

Since the first report by Yamada et al (6), chemoembolization has been performed for inoperable HCCs worldwide. Although the local recurrence rates after chemoembolization have been higher than those after RF ablation (7,8), it can be performed in almost all patients with HCC regardless of the size or number of tumors. However, the prognosis of patients

Departments of Diagnostic Radiology (S.M., M.Y., M.O., Y.Y., N.S. S.I., Y.N.); Internal Medicine (K.N., D.T., N.T.), and Surgery (T.M.), Fukuiken Saiseikai Hospital, 7-1 Funabashi, Wadanakacho, Fukui 918-8503, Japan; and Department of Radiology (O.M.), Kanazawa University Graduate School of Medical Science, Kanazawa, Japan. Received February 11, 2009; final revision received March 8, 2010; accepted April 5, 2010. **Address correspondence to** S.M.; E-mail: s-miyayama@fukui.saiseikai.or.jp

None of the authors have identified a conflict of interest.



DOI: 10.1016/j.jvir.2010.04.015

with large HCC treated by chemoembolization is limited (2,9). Large tumors are usually fed by multiple feeding arteries—not only hepatic arterial branches but also extrahepatic collaterals—and this may make it difficult to achieve complete necrosis of large tumors by chemoembolization (10,11). In a report by Chung et al (11), the prevalence of extrahepatic blood supply at the initial chemoembolization session in a tumor less than 4 cm in diameter was less than 3%; this increased to 63% when the tumor was larger than 6 cm in diameter. For transcatheter management of HCC to be effective, not only the hepatic arterial branches but also these collateral vessels should be adequately embolized (10–13).

We have introduced tumor-targeting chemoembolization for HCC to improve the local control effects and to reduce adverse effects (7,8). In this report, we describe the local therapeutic effects, survival rates, and complications of chemoembolization in the treatment of HCCs larger than 5 cm in diameter.

## MATERIALS AND METHODS

We performed a retrospective study to evaluate the therapeutic effects of chemoembolization for large HCC lesions. This was a retrospective study that used imaging data and clinical records with no change in patient care; institutional review board approval is not required at our institution for this type of study. Written informed consent was obtained from each patient before the chemoembolization procedure.

### Patients

The selection criteria required patients to have (i) HCCs larger than 5 cm in largest diameter, with three or fewer tumors and no portal vein tumor thrombus; and (ii) newly detected HCC without any previous treatment. We excluded patients with more than four lesions or with tumors extending into the portal vein because it was expected to be difficult to perform tumor-targeting chemoembolization in these cases. We also excluded patients with a history of HCC treatment because blood supply to the tumor may have been influenced by the previous treatment. The following conditions were also considered contraindications to chemoembolization: severe thrombocytopenia (platelet count < 30,000/mL), hyperbilirubinemia (serum total bilirubin > 3 mg/dL), and severe hepatic dysfunction (ie, Child-Pugh class C disease). Between March 2000 and July 2008, 30 patients met the listed criteria. There were 23 men and seven women, and the mean patient age (± SD) was 70.4 years ± 8.1 (range, 52–83 y). Patient profiles are summarized in **Table 1**. All patients had chronic hepatitis ($n$ = 2) or liver cirrhosis ($n$ = 28). This was related to hepatitis C virus in 17 patients (56.7%) and hepatitis B virus in three patients (10.0%). The etiology was unknown in 10 patients (33.3%). Twenty-five patients (83.3%) were classed as having Child-Pugh class A disease and five (16.7%) had Child-Pugh class B disease. Twenty-five patients (83.3%) had a solitary tumor and five (16.7%) had two or three tumors. The mean diameter of the largest tumor was 7.7 cm ± 2.4 (range, 5.1–14 cm). Diagnosis was established by imaging findings of computed tomography (CT) and/or magnetic resonance (MR) imaging: characteristic nodular enhancement on the arterial phase and washout on the delayed-phase images. Serum levels of $\alpha$-fetoprotein were more than 21 ng/mL in 12 patients (21–100 ng/mL, $n$ = 6; 101–400 ng/mL; $n$ = 3; and > 401 ng/mL, $n$ = 3). Serum levels of protein induced in vitamin K absence II (14) were more than 41 mAU/mL in 26 patients (41–100 mAU/mL, $n$ = 2; 101–400 mAU/mL, $n$ = 6; > 401 mAU/mL, $n$ = 18). Serum levels of protein induced in vitamin K absence II were not measured in one patient. In 10 patients, serum levels of both tumor markers were increased. In three patients, serum levels of both tumor markers were within the normal ranges. Histologic confirmation was not obtained in any patient. None of the tumors were candidates for surgical resection because of tumor distribution extending to the bilateral lobes or beyond the hepatic hilum ($n$ = 9), poor hepatic function reserve (ie, Child-Pugh class B disease; $n$ = 5), cardiopulmonary dysfunction ($n$ = 4), other underlying diseases ($n$ = 7), or patient refusal ($n$ = 5).

Four patients (13.3%) presented with hemoperitoneum resulting from tumor rupture. Two patients presented with massive bleeding and emergent chemoembolization was performed. In the remaining two patients with minor bleeding, chemoembolization was electively performed. In another patient (3.3%) with a tumor measuring 14 cm in diameter, serum total bilirubin level was increased to 12.8 mg/dL as a result of bile duct compression at the hepatic hilus by the tumor. Chemoembolization was performed after normalization of serum bilirubin level after percutaneous transhepatic biliary drainage.

**Table 1**
**Patient and Disease Profile ($N$ = 30)**

| Characteristic | Value |
|---|---|
| Sex | |
| Male | 23 |
| Female | 7 |
| Mean age (y) | 70 ± 8.1 |
| Liver cirrhosis | 28 (93.3) |
| Chronic hepatitis | 2 (6.7) |
| Hepatitis C virus–related | 17 (56.7) |
| Hepatitis B virus–related | 3 (10.0) |
| Etiology unknown | 10 (33.3) |
| Mean maximum HCC size (cm) | 7.7 ± 2.4 |
| Intrahepatic multiplicity | |
| Single | 25 (83.3) |
| Multiple (≤ 3) | 5 (16.7) |
| Tumor rupture | 4 (13.3) |
| Obstructive jaundice | 1 (3.3) |

Note.—Values in parentheses are percentages. Values presented as means ± SD where applicable.

### Chemoembolization Technique

A 2-F–tip (Progreat-$\alpha$; Terumo, Tokyo, Japan) or 2.4-F–tip (Microferret; Cook, Bloomington, Indiana) microcatheter was used for all chemoembolization procedures through a 4-F catheter placed in the celiac artery, superior mesenteric artery, or common hepatic artery. To navigate the microcatheter, a 0.016-inch guide wire (GT-wire; Terumo) was used. The microcatheter was advanced into the tumor-feeding branch as selectively as possible to minimize the embolized area in each patient.

After the microcatheter was inserted into the target branch, 0.5 mL of 2% lidocaine (Xylocaine; Fujisawa,

Osaka, Japan) was intraarterially injected to prevent pain and vasospasm. First, a mixture of iodized oil (Lipiodol; Laboratoire Andre Guerbet, Aulnay-sous-Bois, France) and anticancer drugs was injected and injection of gelatin sponge particles followed. The total amount of iodized oil in the single procedure was determined based on the tumor size (almost equal to the diameter of the tumor, eg, a 6-cm tumor received 6 mL of iodized oil), but did not exceed 10 mL. In total, 6–10 mL of iodized oil, 30 mg of epirubicin (Farmorbicin; Kyowa Hakko, Tokyo, Japan), and 6 mg of mitomycin C (Kyowa Hakko) were used in a single procedure. After injecting the mixture of iodized oil and anticancer drugs, the target branch was embolized by gelatin sponge particles until the blood flow was stopped. Until December 2006, gelatin sponge particles (Gelfoam; Upjohn, Kalamazoo, Michigan) that had been cut into approximately 1-mm cubes were injected to block the target vessel. Since January 2007, commercially available gelatin sponge particles (Gelpart; Nippon Kayaku, Tokyo, Japan) 1 mm in diameter were used. When the tumor was extremely large or had multiple feeding arteries, stepwise chemoembolization sessions were performed at 3–10-week intervals to avoid complications. In addition, extrahepatic collateral vessels supplying the tumor were identified and embolized if necessary. Arteriograms of the right inferior phrenic artery (IPA) and right renal capsular artery were routinely obtained in almost all patients. Other extrahepatic collateral vessels, such as the left IPA, right intercostal and lumbar arteries, right adrenal arteries, and bilateral internal mammary arteries, were examined according to the tumor location. Aortography was not performed in any patient in this series.

### Follow-up

Unenhanced CT was performed 1 week after the procedure in all patients to check for iodized oil accumulation in the target tumor. All patients were followed by dynamic CT and/or MR imaging every 2–3 months after chemoembolization to screen for any tumor recurrence. In patients who underwent stepwise chemoembolization sessions, follow-up dynamic CT and/or MR imaging studies were obtained every 2–3 months after the last session of the sequential treatment. When tumor recurrence and/or newly developed tumors at other sites were detected, additional chemoembolization was performed if possible. Intraarterial infusion chemotherapy was indicated for patients when intrahepatic disseminated lesions became uncontrollable by chemoembolization. Distant metastases that developed in patients with controlled HCC in the liver were treated by combined chemoembolization and radiation therapy.

### Assessments

Early tumor response was assessed by dynamic CT or MR imaging obtained 2–3 months after the initial treatment based on the change in the maximum diameter of the whole tumor, according to the criteria of Response Evaluation Criteria In Solid Tumors (15). Overall survival rates and progression-free survival rates were calculated by the Kaplan-Meier method.

Major complications were assessed based on the previously described guideline for transhepatic arterial chemoembolization, embolization, and chemotherapeutic infusion for hepatic malignancy (16).

## RESULTS

### Treatment

In 20 patients (66.7%) with a mean maximum tumor diameter of 6.6 cm ± 1.5 (range, 5.1–10 cm), including four who had a ruptured tumor, the tumor was embolized in a single chemoembolization procedure. In the remaining 10 patients (33.3%) with a mean maximum tumor diameter of 10 cm ± 2.2 (range, 7.2–14 cm), two– to four–stepwise chemoembolization sessions (mean, 2.7 sessions ± 0.8) were performed per patient.

In 24 patients (80.0%), multiple chemoembolization procedures were performed during the subsequent treatment course. The total number of mean chemoembolization sessions in each patient was 4.0 sessions ± 3.0 (range, 1–13 sessions).

Three patients underwent another treatment in addition to chemoembolization. Two patients underwent implantation of an arterial infusion port system because of uncontrollable intrahepatic metastases and underwent infusion of 2,500 mg of 5-fluorouracil (Kyowa Hakko) on day 1. Interferon (12 million IU; Advaferon; Astellas, Tokyo, Japan) was also subcutaneously administered on days 1, 3, and 7. This treatment schedule was repeated twice in one patient and four times in another at 1-week intervals; however, it was not effective. Bone metastasis to the left seventh rib developed in another patient with well controlled HCC in the liver, and the metastatic lesion was treated by a combination of chemoembolization with 20 mg of epirubicin and gelatin sponge particles followed by 50 Gy of radiation therapy. However, bone metastases at other sites rapidly developed in this patient.

### Chemoembolization through Extrahepatic Collateral Vessels

Extrahepatic blood supply to the largest tumor was observed in 21 patients (70.0%) during the treatment course. In particular, this finding was observed in 14 patients (46.7%) at the initial chemoembolization (**Fig 1**). In total, 62 collateral vessels that fed the tumor were demonstrated during the observation period, including 22 vessels at the initial procedure. All vessels were successfully embolized with use of a mixture of iodized oil and anticancer drugs and gelatin sponge particles (**Table 2**).

### Local Tumor Control

**Table 3** shows local tumor control of each tumor after chemoembolization. In 28 patients (93.3%), the entire tumor could be completely embolized as shown on arteriograms, including those treated by intentional stepwise chemoembolization. In all four patients with ruptured tumor, hemostasis was achieved by chemoembolization. Concerning early tumor response 2–3 months after treatment as assessed by Response Evaluation Criteria In Solid Tumors, 13 patients (43.3%) were classified as having a partial response, 16 patients (53.3%) were classified as having stable disease, and one patient (3.3%) was classified as having progressive disease. Complete response was not achieved in any patient (0%),

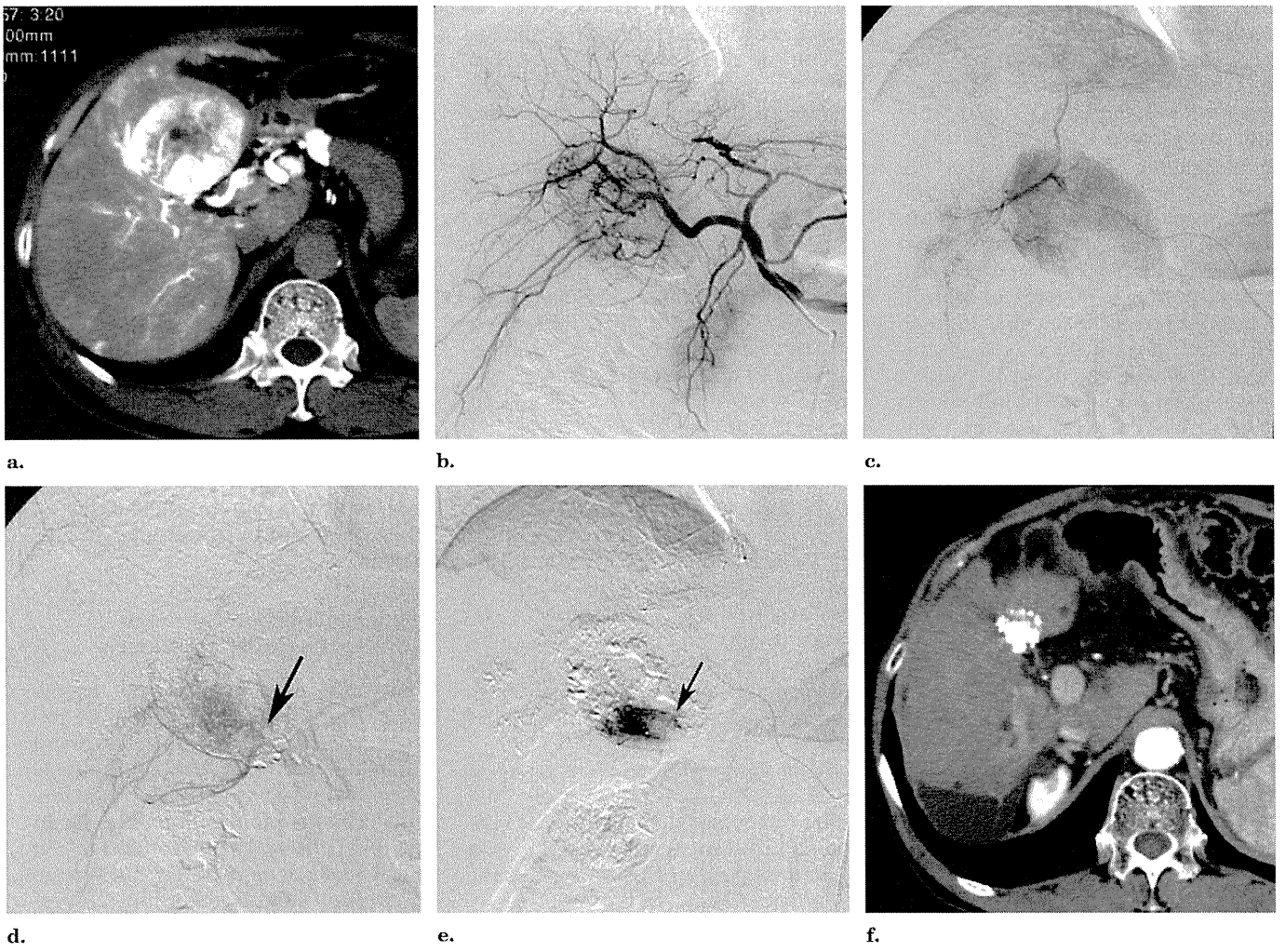


**Figure 1.** Images from a 66-year-old man with HCC 7.6 cm in diameter. **(a)** Axial CT during hepatic arteriography showed a large hypervascular tumor in segments IV and V of the liver. **(b)** Celiac arteriogram showed a large tumor stain. **(c)** First, the anterior segmental artery of the liver was selected and chemoembolization was performed. **(d)** Arteriogram of the cystic artery obtained after chemoembolization of the anterior segmental artery showed a partial tumor stain. The arrow indicates the tumor-feeding branch. **(e)** The tumor-feeding branch was selected and chemoembolization was performed. The arrow indicates the catheter tip. Seven weeks later, chemoembolization through the medial segmental artery of the liver was performed (not shown). The tumor recurred after 6 and 77 months and was treated by chemoembolization. A new lesion that developed after 63 months was also treated by chemoembolization (not shown). **(f)** Axial CT scan obtained 102 months after the initial chemoembolization shows that tumor size is markedly reduced. There are no viable tumors detected in the liver.

Therefore, the early response rate was 43.3%.

In 11 of 28 patients, complete radiologic response was achieved during the follow-up period of 6–103 months (mean, 32.6 months ± 22.3; **Figs 1, 2**). In one patient, a 6-cm-diameter tumor disappeared 11 months after a single chemoembolization (**Fig 2**).

In 17 of 28 patients, local tumor progression was observed within 2–77 months (mean, 12.9 months ± 17.9) and additional chemoembolization was performed. In this group, complete radiologic response was achieved in eight of 17 patients. In nine patients, the tumor progressed despite repeat chemoembolization (**Fig 3**).

In the remaining two patients, who had maximum tumor diameters of 9.3 cm and 14 cm, respectively, the entire tumor could not be completely embolized despite stepwise chemoembolization. In both patients, residual tumor stain was observed through the left hepatic artery at the end of the fourth and final chemoembolization procedure performed through the right hepatic artery. Additional chemoembolization could not be performed in either patient because of poor general condition.

Tumor recurrence at other sites in the liver was also observed in 16 patients (53.3%), and was treated by chemoembolization if possible.

## Outcomes

All patients were followed up for 4–103 months (mean, 33.8 months ± 24.1). Eleven patients (36.7%) died during a follow-up of 4–61 months (mean, 27.2 months ± 21.8). Seven patients (23.3%) died of tumor progres-

**Table 2**
**Incidences of Blood Supply to HCC from Extrahepatic Collateral Vessels**

| Artery | During Follow-up ($n$ = 21; 70.0%) | At Initial Treatment ($n$ = 14; 46.7%) |
|---|---|---|
| Right inferior phrenic | 14 | 6 |
| Cystic | 6 | 3* |
| Right renal capsular | 6 | 2 |
| Left inferior phrenic | 6 | 1 |
| Right posterior intercostal | 4 | 1 |
| Right omental | 4 | 2 |
| Right middle adrenal | 4 | — |
| Left gastric | 4 | 1 |
| Right internal mammary | 3 | 2 |
| Bile duct | 2 | 1 |
| Right colic | 2 | — |
| Dorsal pancreatic | 2 | 1 |
| Right gastric | 1 | 1 |
| Right inferior adrenal | 1 | — |
| Middle colic | 1 | — |
| Right lumbar | 1 | — |
| Left gastroepiploic | 1 | 1 |
| Total | 62 | 22 |

* Cholecystitis occurred as a result of the development of a fistula between the tumor and the gallbladder after chemoembolization through the cystic artery in one patient.

**Table 3**
**Outcomes on a Per-tumor and Per-patient Basis**

| Outcome | Incidence |
|---|---|
| Per tumor ($N$ = 30) | |
| Successful treatment of entire tumor(s) | 28 (93.3) |
| Complete remission after initial treatment | 11 (33.3) |
| Local tumor recurrence | 17 (56.7) |
| Complete remission after additional procedure(s) | 8 (26.7) |
| Local recurrence despite additional procedure(s) | 9 (30.0) |
| Unsuccessful treatment of entire tumor(s) | 2 (15.0) |
| Newly developed tumor(s) at other site(s) | 16 (53.3) |
| Per patient ($N$ = 30) | |
| Dead | 11 (36.7) |
| Mean survival (mo) | 27.2 ± 21.8 |
| Tumor progression | 7 (23.3) |
| Causes unrelated to liver | 4 (13.3) |
| Alive | 19 (63.3) |
| Mean survival (mo) | 37.5 ± 25.2 |
| Without viable tumor | 14 (46.7) |
| With viable tumor | 5 (16.7) |

Note.—Values in parentheses are percentages. Values presented as means ± SD where applicable.

sion, including distant metastases (lung, $n$ = 2; bone, $n$ = 2). Four deaths (13.3%) were unrelated to hepatic causes: arrhythmia after 4 months, pneumonia after 7 months, infectious endocarditis after 54 months, and massive bleeding from a gastric ulcer after 61 months. Two of these patients (one with a tumor measuring 8.6 cm in diameter who died 4 months later, and another with a tumor measuring 10 cm in diameter who died 61 months later) had no viable HCC at the time of death. One patient who died after 7 months had a small viable portion in the tumor measuring 14 cm in diameter, and the remaining patient who died after 54 months had a new small tumor without local progression of the initial tumor measuring 10 cm in diameter. Nineteen patients (63.3%) survived for 6–103 months (mean, 37.5 months ± 25.2). Sixteen patients did not exhibit any viable tumors on the last follow-up CT images obtained 6–102 months after treatment (mean, 40.5 months ± 6.6). Three patients had viable HCC on the last follow-up CT study obtained 15, 19, and 27 months after treatment, respectively. Two of three patients had a locally progressed tumor (**Fig 3**). The remaining patient had intraperitoneal seeding masses in addition to a locally progressed tumor and intrahepatic metastases because this patient had presented with tumor rupture before chemoembolization. The cumulative overall survival rates at 1, 2, 3, 4, 5, and 6 years were 82.3% (95% CI, 82.6%–96.4%), 78.5% (95% CI, 63.2%–93.8%), 73.9% (95% CI, 57.0%–90.8%), 73.9% (95% CI, 57%–90.8%), 49.3% (95% CI, 23.4%–75.2%), and 32.9% (95% CI, 1.5%–64.3%), respectively. The progression-free survival rates at 1, 2, 3, 4, 5, and 6 years were 66.0% (95% CI, 48.8%–83.3%), 57.6% (95% CI, 39.0%–76.2%), 57.6% (95% CI, 39.0%–76.2%), 51.2% (95% CI, 30.8%–71.6%), 51.2% (95% CI, 30.8%–71.6%), and 34.2% (95% CI, 3.6%–64.8%), respectively (**Fig 4**). The median survival was 4.5 years ± 0.5.

## Complications

There were three major complications (10%) that were successfully managed by percutaneous drainage. In one patient who underwent percutaneous transhepatic biliary drainage before chemoembolization, infection to the necrotic tumor and fistula between the tumor and bile duct developed. The biliary drain was left in place after removal of the drainage tube in the necrotic tumor cavity until the patient died of pneumonia 7 months after the initial chemoembolization procedure. In another patient with a tumor that invaded the gallbladder, cholecystitis occurred as a result of the development of a fistula between the tumor and gallbladder. In this patient, the tumor was initially fed by the cystic artery and the feeding branch derived from the cystic artery was embolized. Percutaneous transhepatic gallbladder drainage was performed and the drainage tube was removed after cholecystitis was resolved. In the remaining patient, who


**Figure 2.** Images from an 81-year-old woman with HCC 6 cm in diameter. **(a)** Axial arterial-phase CT showed a tumor in segments XI and XII (arrow). **(b)** The tumor-feeding branch was selected and chemoembolization was performed. **(c)** Axial CT image obtained 1 week after chemoembolization showed dense iodized oil accumulation in the tumor. **(d)** The tumor disappeared 11 months after chemoembolization. Axial CT image obtained 3 years and 7 months after chemoembolization shows that the tumor disappeared, and a small amount of iodized oil is still retained in the liver parenchyma (arrow).

presented with dilation of the intrahepatic bile duct caused by compression of the tumor before chemoembolization, a large biloma developed after three chemoembolization sessions including embolization of the caudate arterial branches of the liver, and it was treated by percutaneous drainage. After healing of the biloma, obstructive jaundice caused by the bile duct stricture at the hepatic hilus also developed. Percutaneous transhepatic biliary drainage was performed and the bile duct stricture was managed by placement of two metallic stents (Zilver stent; Cook; **Fig 3**). There were no toxic complications as a result of injection of anticancer drugs in any patient.

## DISCUSSION

Treatment for large HCCs is challenging. For small unresectable HCCs less than 3 cm in diameter, several local therapeutic options are available, such as RF ablation (3–5), microwave coagulation (17), ethanol injection (18), or acetic acid injection (19), in addition to chemoembolization (6–9). However, local therapies may have limited effects on medium and large HCCs (4,5).

Tumor size is one of the most important predictive factors for long-term prognosis after hepatectomy (20). According to the report from the Liver Cancer Study Group of Japan (1), the survival rates for patients with a maximum tumor diameter greater than 5 cm but less than 10 cm treated by surgical resection were 81%, 56%, and 42% at 1, 3, and 5 years, respectively, and those in patients with a maximum tumor diameter greater than 10 cm treated by surgical resection were 67%, 43%, and 32% at 1, 3, and 5 years, respectively. Shuto et al (21) reported that the 1-, 5-, and 10-year tumor-free survival rates in patients with tumors larger than 5 cm in diameter treated by hepatic resection were 48%, 18%, and 16%, respectively.

There are a few reports concerning nonsurgical treatment of large HCCs. Livraghi et al (5) reported the usefulness of RF ablation for HCCs larger than 5 cm in diameter, indicating that 100% tumor necrosis was achieved in 25% of noninfiltrating tumors and 23% of infiltrating tumors, and 90% or more necrosis was achieved in 71% of noninfiltrating tumors and 59% of infiltrating tumors. However, in a report by Obara et al (22), insufficient treatment of HCC by RF ablation, which allows the survival of some tumor cells, might induce further malignant transformation in vivo. Osuga et al (23) reported bland embolization with the use of superabsorbent polymer microspheres for large HCCs with a mean diameter of 8.1 cm, and complete necrosis was achieved in three of nine tumors, nearly complete necrosis (90%–99%) was achieved in three, and partial necrosis (50%–90%) was achieved in three. Takaki et al (24) reported RF ablation combined with chemoembolization for 20 patients with 32 HCCs larger than 5 cm in diameter (mean maximal tumor diameter of 6.2 cm) who each had fewer than three lesions. Their estimated overall survival rates were 100%, 62%, and 41% at 1, 3, and 5 years, respectively. In the present study, overall and progression-free survival rates at 1, 3, and 6 years were 82.3% and 66.0%, 73.9% and 57.6%, and 32.9% and 34.2%, respectively. This suggests that chemoembolization for large HCCs may also be an effective therapeutic option, although multiple procedures are required.

Severe complications after chemoem-